International Journal of Humanoid Robotics
Vol. 13, No. 2 (2016) 1550033 (30 pages)

DOI: 10.1142/S0219843615500334

Determining the Important Subjective Criteria in the Perception of Human-Like Robot Movements Using Virtual Reality

Olivier Hugues[*,§], Vincent Weistroffer[*,¶], Alexis Paljic[*,‖],
Philippe Fuchs[*,**], Ahmad Abdul Karim[†,††], Thibaut Gaudin[†,‡‡]
and Axel Buendia[†,‡,§§]

[*]*MINES ParisTech, PSL Research University*
Center for Robotics, Paris, France

[†]*SPIR.OPS, Scientific Research Lab, Paris, France*

[‡]*CNAM CEDRIC, Paris, France*
[§]*oliver.hugues@mines-paristech.fr*
[¶]*vincent.weistroffer@mines-paristech.fr*
[‖]*alexis.paljic@mines-paristech.fr*
[**]*philippe.fuchs@mines-paristech.fr*
[††]*ahmad.abdul.karim@spirops.com*
[‡‡]*thibaut.gaudin@spirops.com*
[§§]*axel.buendia@spirops.com*

Received 31 July 2014
Accepted 19 May 2015
Published 7 July 2015

This paper deals with the design and the evaluation of human-like robot movements. Three criteria were proposed and evaluated regarding their impact on the human-likeness of the robot movements: The inertia of the base, the inertia of the end-effector and the velocity profile. A specific tool was designed to generate different levels of anthropomorphism according to these three parameters. An industrial use case was designed to compare several robot movements. This use case was implemented with a virtual robot arm in a virtual environment, using virtual reality. A user study was conducted to determine what were the important criteria in the perception of human-like robot movements and what were their correlations with other notions such as safety and preference. The results showed that inertia on the end-effector was of most importance for a movement to be perceived as human-like and nonaggressive, and that those characteristics helped the users feel safer, less stressed and more willing to work with the robot.

Keywords: Human–robot interaction; robot movements; human-like movements; virtual reality.

1. Introduction

Human–robot interaction studies the way people and robots interact with each other.[1] The interaction may be simple, like observing robots, being next to them or communicating with them. This interaction nowadays is becoming more complex, especially with people and robots collaborating with each other on a daily basis in some industrial tasks.[2] Human–robot collaboration, in the context of the industry, faces specific needs and challenges in terms of safety or efficiency. Since people and robots tend to be closer to each other and to work together, it is important to know how robots are perceived and accepted by people in their environment.

One important question is to know whether robots are better accepted if they behave like humans. Several factors have to be taken into account, such as robot appearance, robot movements or their overall interaction with people.[3] In this paper, we focus on robot movements. Available studies in the literature lead us to better understand how to generate human-like robot movements using inverse dynamics,[4] human motion imitation[5] or with geometric constraints,[6] but many questions remain unanswered. Because a human-like robot movement is sometimes hard to implement in real conditions, we propose to breakdown robot movements into multiple factors (three parameters will be proposed) and to study the effects of these parameters.

First, we are interested in determining the important criteria that make a robot movements human–like. Secondly, using these criteria, we want to know if human-like movements generated by our criteria are indeed better accepted by people, in terms of safety and the will to work with them. In this context, a specific tool was implemented to generate different levels of anthropomorphism on industrial robotic arms, and a user study was conducted to gather people' subjective impressions.

In Sec. 2, we present related work on the generation of human-like movements and their perception on robots. In Sec. 3, we describe the tool that was implemented to generate human-like robot movements. Section 4 presents the use case, the different levels of anthropomorphism and the user study that was conducted. The results of this study are described in Sec. 5, before giving a short conclusion in Sec. 6.

2. Related Work on Robot Movements Evaluation

The study of the acceptability of human–robot interaction and collaboration has generally focused on several factors, which include robot appearance,[7] robot movements,[8] and more importantly anthropomorphism.[9] Making a robot capable of acting as a human is a large field which involves developments of computationally-based representation, modeling, control, and animation of human movement.[10]

Duffy[9] defined anthropomorphism as "the tendency to attribute human characteristics to inanimate objects, animals and others with a view to helping us rationalize their actions". Concerning robot appearance, the question is to know if a humanoid robot is better accepted than a machine-looking one: Mori[11] asserted that it was true until a certain point was reached, when incomplete or awkward details were too disturbing. This phenomenon was called the uncanny valley, and several studies tried to confirm or discredit it. Psychological aspects were underlined in these studies showing, for example, the gap when humans start to attribute human-like cognitive processes to the robot.[12] Concerning robot movements, the idea is to know if human-like movements are better perceived than machine-like ones.

It is not easy to determine what a human-like movement is. Several studies tried to highlight invariant characteristics of the human motion. Morasso[13] studied point-to-point movements of the human hand and observed that the hand trajectories were always straight lines with a single peaked tangential velocity curve. Viviani and Terzuolo[14] observed that, in the writing movements of the human hand, there was an invariant relation between the angular velocity and the curvature of the hand's trajectory. Those invariants may be characteristics of a biological motion, and Johansson[15] showed that the human visual perception was sensitive to those invariants: People were able to discern a biological motion described only by a few moving bright spots.

Even if invariants of the biological motion exist, it is another problem to model them. Many studies used their own human-like movements algorithms designed with a wide range of approaches. Some studies generated biological motion by minimizing the trajectory's jerk,[16] others by minimizing the torques' rate of change.[17] Additional studies also used the two-thirds power law to generate human-like movements.[18] Finally, Taïx *et al.*[19] used a computational approach with optimal, Saab *et al.*[4] used inverse dynamics, while Suleiman *et al.*[5] used human motion capture.

The generation and perception of human-like movements on robots has been the focus of a lot of studies. Shibata and Inooka[8] used an industrial robot with different velocity profiles to examine which factors were essential for human-likeness. Huber *et al.*[20] compared two velocity profiles (trapezoidal joint and minimum-jerk) in a human-robot handing-over task, in terms of human-likeness and safety. Kulić and Croft[21] and Zanchettin *et al.*[22] estimated the human affective state in front of different robot motion strategies (human-like or not). Weistroffer *et al.*[23] studied if the perception of human-like movements depended on the robot appearance. Another study showed that "the naturalness judgments did not completely indicate the perception of movement".[24] It was also shown that, for humanoid robots, rapid movements had a negative impact on naturalness. Co-verbal gestures have also been studied showing that nonverbal behaviors which affect anthropomorphism perception.[25]

On the whole, those studies focused on specific robot movement profiles, determined how much they were perceived human-like and drew interesting results on their correlation with other notions, such as pleasantness, safety, or efficiency. But there were sparse details to explain which part of the motion was responsible for its human-likeness: Was it the end-effector trajectory, its speed or the overall structure of the movement? In this paper, we wanted to determine what were the important subjective criteria for an industrial robot's movements to be perceived as human-like. We also wanted to know their correlations with other notions such as safety, competence and the will to work with them. In this context, different levels of anthropomorphic robot motions were generated, thanks to specific algorithms. An industrial use case was designed and a user study was conducted to gather subjective impressions on the different robot motions.

3. Human-Like Movements Generation

3.1. *Inverse kinematics overview and techniques*

To generate different robot arm movements for our study, **Inverse Kinematics** (IK) methods can be used. An IK problem can be explained as follows: In an articulated chain the generalized location of an end-effector e (the joint at the end of a chain of joints) is a function of the rotations of all joints Joint_i in that chain (see Fig. 1).

$$e = f(\text{Joint}). \tag{1}$$

A typical IK problem is calculating these joints' rotations using only the location of the end-effector: Given a desired position (Target), what must be the angles of the skeleton's joints?

$$\text{Joint} = f^{-1}(\text{Target}). \tag{2}$$

Equation (2) may not always have a (unique) solution. Indeed, there are multiple and sometimes endless combinations of joint degrees of freedom (DOF) values that put the end-effector in the right location. Van Welbergen *et al.*[26] identified several numerical techniques to solve this problem: *Analytical* IK systems, *Data-Based* IK systems and *Mesh-Based* techniques.

Analytical IK systems, like the **Jacobian Inverse** method used in Refs. 27 and 28, use an iterative method that tries to approximate a good solution using the relation between the joint velocities and the velocity of the end-effector. The **Cyclic Coordinate Descent (CCD)** method proposed in Refs. 29 and 30 iterates through the joints, typically starting with the one closest to the end-effector and cycling through one joint variable at a time according to a heuristic.

Data-Based IK systems use motion data (motion capture or keyframe data) to automatically learn a model of logical and natural poses.[31–34] The goal of this kind of systems is to generate the most natural poses: Poses that are most similar to the space of poses in the training data.

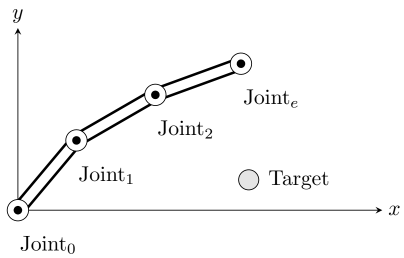

Fig. 1. Example of an IK problem: Given the desired position of a skeleton's hand (Target), what must be the angles of the skeleton's joints?

Finally, *Mesh-Based* IK techniques, like in Refs. 35 and 36, directly move the vertices and polygons of the three-dimensional (3D) model in order to deform the mesh toward the needed position.

3.2. *Spir.Ops tool overview*

In order to generate human-like movements for different robot arms, an IK system capable of generating believable movements is necessary and must be customizable enough to give the possibility to change anthropomorphic parameters based on the needed tests. Most off-the-shelf IK systems do not offer these possibilities. For our study, Spir.Ops[a] created an anthropomorphic geometric-based IK system specific to our needs with a curve following tool to animate 6-DOF (Fig. 2(b)), 7-DOF (Fig. 2(a)) and 15-DOF (Fig. 2(c)) robot arms. Figure 3 shows the tool's viewer.

3.3. *Curve following*

In Spir.Ops tool, we use cubic Hermite splines to represent the trajectories that each robot arm follows. A Hermite curve is a third-degree spline with each polynomial of the spline in Hermite form. The Hermite form consists of two control points and two control tangents for each polynomial. Hermite curves (Fig. 4) are used to smoothly interpolate data between key-points like object movement in keyframe animation or camera control. In our case, we use several Hermite curves to smoothly connect 3D waypoints to produce our final 3D trajectory.

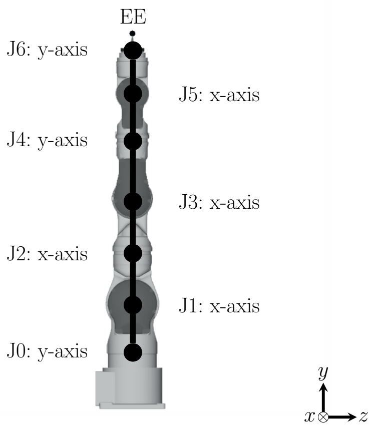

(a) Robot with 7-DOF

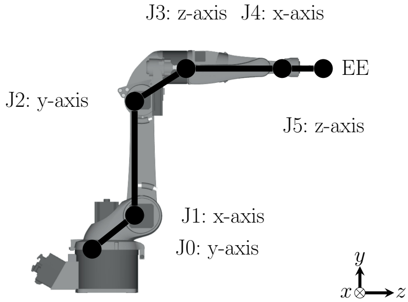

(b) Robot with 6-DOF

Fig. 2. Robots types with their DOF.

[a] Spir.Ops is a private scientific research lab focused on artificial intelligence and procedural animation issues.

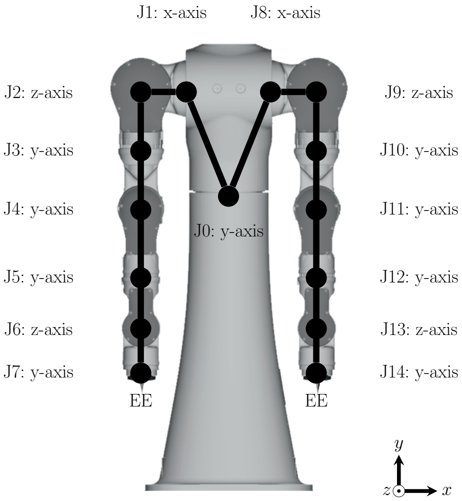

(c) Robot with 15-DOF

Fig. 2. (*Continued*)

In order to travel our final 3D trajectory curve using a needed velocity (distance d in Fig. 4), we sample each Hermite curve (300 sample in our case), and we use these samples as an approximation of each curve.

The velocity profile in our system can be either linear, or in the case of an anthropomorphic control we use the two-thirds power law to control this velocity.[18] Two-thirds power law is an interesting property of the human hand curved

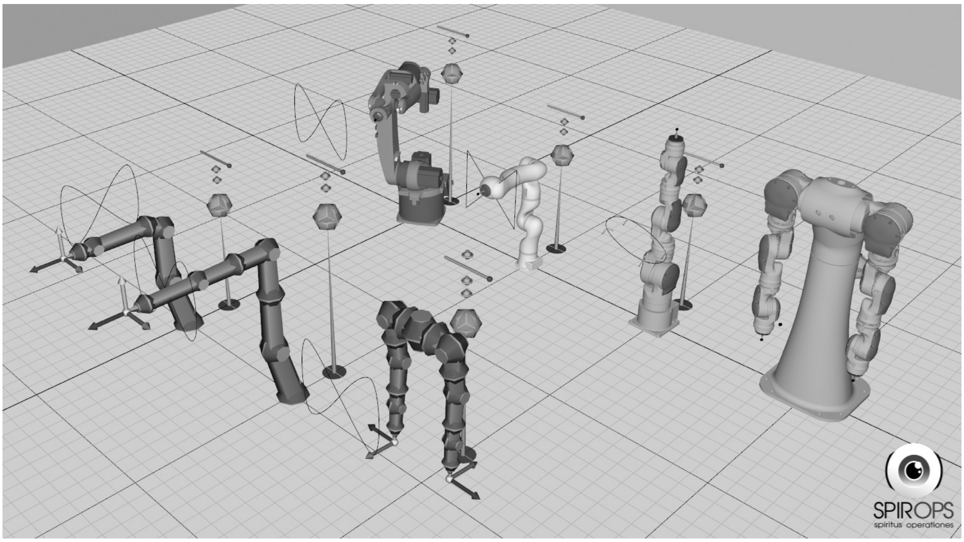

Fig. 3. The viewer of the tool: Different robot structures can be managed.

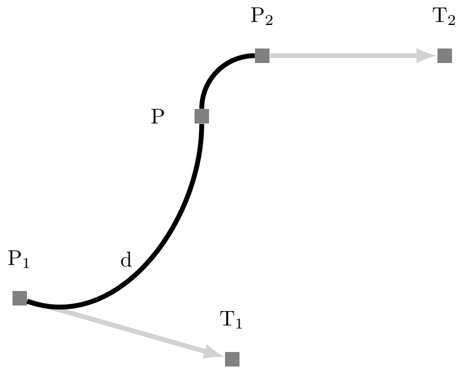

Fig. 4. Hermite curve. P_1, P_2: control points. T_1, T_2: tangents. P: interpolated points. d: needed distance.

movement stating that the speed v of the hand movement on a curve is related to the curvature c of the curve through a power law.

$$v = k \cdot c^{\frac{2}{3}}. \tag{3}$$

Equation 3 is a two-thirds power law where k is the velocity gain factor, accounting for differences in average movement velocity ($k = \frac{1}{3}$ in our system).

3.4. *Anthropomorphic geometric-based IK system*

As we are dealing with specific robot types (see Fig. 3), we created a specific geometric-based IK system that could be seen as less generic than off-the-shelf IK systems, but which at the same time is built around anthropomorphic modifiers which makes it powerful for the needed study.

Our system uses simple 3D geometric equations to find the joint angles of Eqs. (1) and (2). It is not iterative-based making it quite fast (performance wise): We calculate the needed angles for each Joint_i directly without any try-and-error passes, as we will see later in this section.

First, we explain the used calculation steps and the anthropomorphic modifiers with the 7-DOF robot (see Fig. 2(a)). Then, we generalize to the other robots.

3.4.1. *Basic steps*

As all joints are aligned (no translation on the x-axis, Fig. 2(a)), we combine joints in 3 groups (see Fig. 5): Shoulder, Elbow, and Wrist (which contains the end-effector). We do so to simplify our geometric problem and to have a human-like arm structure.

The component Joint_0 of our robot shoulder is the one responsible for orienting the arm toward the target. We call the components Joint_2 and Joint_4, in the shoulder and in the wrist (respectively), the twist components. Joint_6 is a redundant twist used in case of an external constraint to make sure that the end-effector twist is

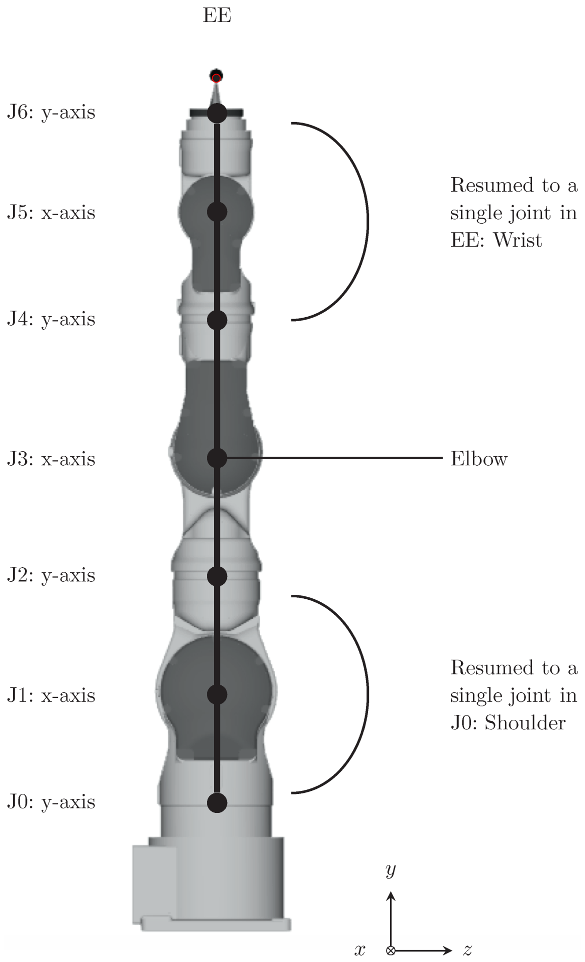

Fig. 5. The simplification used to help solving our IK problem.

correct. Now, starting from the current robot arm position, the basic IK steps are the following:

- Step-1: Using the atan2 function, we calculate Joint_0 angle in order for the robot to face the needed target.
- Step-2: Using circles intersections equations (see Fig. 6), we calculate Joint_1 and Joint_3 values in order to place the Elbow joint Joint_3 on the selected intersection point.

With only these two steps, the end-effector points exactly at the needed target but: Some DOF (Joint) are not yet used and this robot animation is not yet customizable.

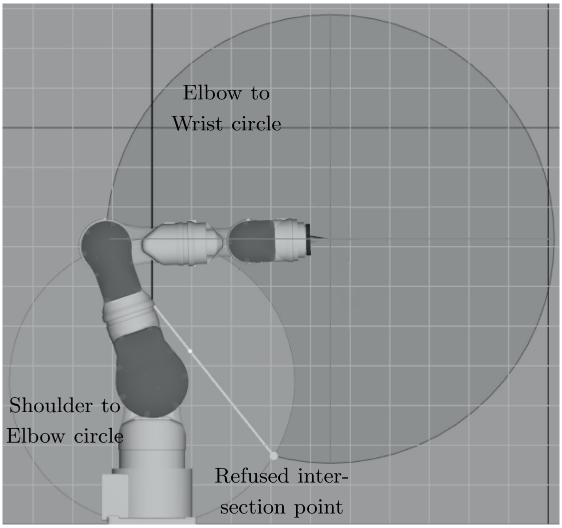

Fig. 6. An example of the intersection circles used to calculate the needed Elbow position so the end-effector reaches the target.

3.4.2. *Adding base inertia*

In **Step-1**, our IK system calculates the final angle (θ_f) in order for Joint_0 to face the target. This order is executed directly and the Joint_0 of the IK chain turns instantly.

To make the base joint movement smoother, with a more organic feeling, we added an inertia on Joint_0 movement using a spring damper. This inertia component adds a controlled delay when Joint_0 executes the commands of our IK system. In this way, Joint_0 converges toward the needed final angle θ_f in t time based on the used spring damper regime (and not instantly). This changes our IK system as follows:

(1) Our IK System calculates a θ_f for Joint_0 (**Step-1**).
(2) The spring damper interpolates between current angle θ_c and θ_f based on its regime given us a θ_n.
(3) We apply this θ_n on our Joint_0.
(4) In **Step-2**, the IK system starts with $\text{Joint}_0 = \theta_n$ now, so it calculates Joint_2 and Joint_4 values to compensate for this new delay, adding new twists on our animated chain.

In order to timely control the movement of this spring damper, we use the Settling Time τ_s principle, like in Abdul Karim *et al.*,[37] as follows: Let m be a mass connected to a spring with stiffness constant k. This mass oscillates around a rest position x_0 with a viscous damper that has a damping coefficient c. Based on Newton's second law of physics the acceleration is $\ddot{x} = -(k(x - x_0) + c\dot{x})/m$ where x is the current position of the mass and $\dot{x}$ is its velocity. The mass m oscillates around the rest value x_0, seeking to minimize the error $(x - x_0)$ until reaching zero. This oscillation depends

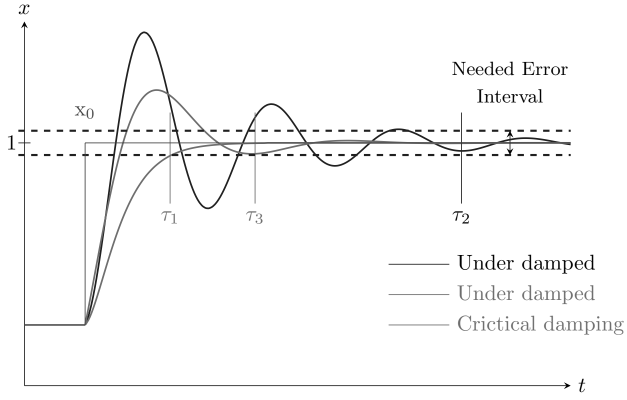

Fig. 7. Spring oscillation under different damping values.

directly on the constants (k, c, m). The Settling Time τ_s is the time required for the mass position x to reach its maximum amplitude inside a given error interval (see Fig. 7) and remain inside it. This interval is symmetrical around x_0.

$$\tau_s = -\frac{\ln(\text{tolerance fraction})}{\zeta * w_0}. \tag{4}$$

In Eq. (4), the tolerance fraction is the needed error interval shown in Fig. 7, w_0 is the natural frequency and ζ is the damping of the ordinary differential equation governing a damped harmonic oscillator:

$$m\ddot{x} + c\dot{x} + k(x - x_0) = 0,$$

or

$$\ddot{x} + 2 * \zeta * w_0 * \dot{x} + w_0^2 * (x - x_0) = 0,$$

with

$$\zeta = \frac{c}{2mw_0}, \quad w_0 = \sqrt{\frac{k}{m}}. \tag{5}$$

By fixing the tolerance fraction to 5% in Eq. (4) and by using the user provided settling time and damping (underdamped most of the time with a value of 0.7), the spring damper constants k and c are calculated from Eq. (5), achieving total control over the curve of the spring damper while maintaining its dynamic aspect.

Even with the addition of the **Base Inertia**, the resulting wrist movement is still static (Joint_5 is not animated yet) and the wrist only reacts to the base joint delay if it is active (the calculated twist on Joint_4). It is like if the movement is driven by the base Joint_0, while, normally, the wrist (with the end-effector) is the most important component and the one that should be driving the whole articulated chain motion toward the target. So first, we add the ability to control the wrist Joint_5 angle

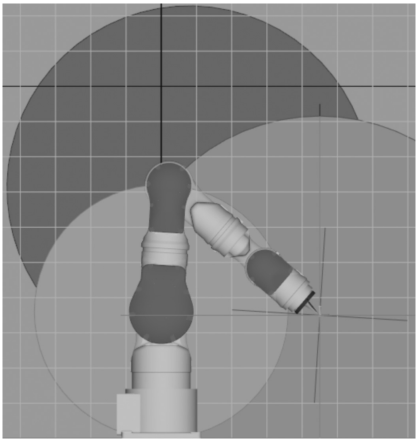

(a) The first IK steps.

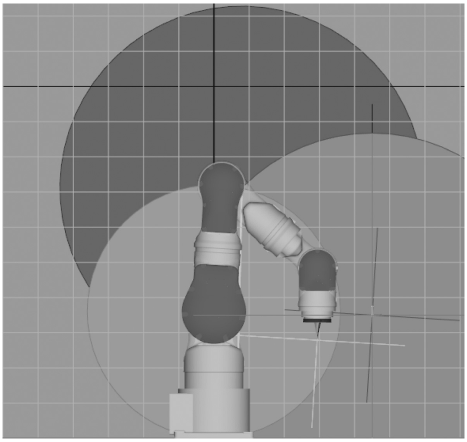

(b) The needed Joint angle resulting in a new Elbow-wrist Circle (in blue).

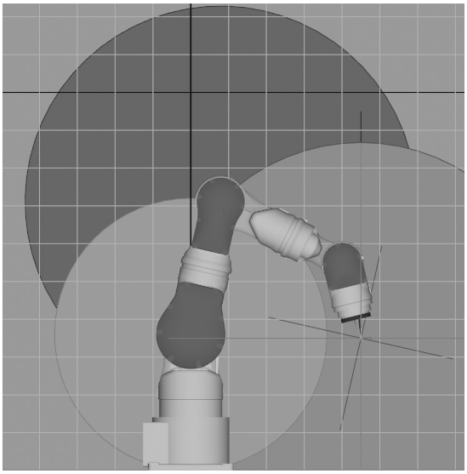

(c) We adapt $Joint_1$ and $Joint_3$ to the new circle using the same circles intersections equations in Step-2.

Fig. 8. Direct wrist control using an external $Joint_5$ angle.

independently as illustrated in Fig. 6. We go through the previous IK steps as before (Fig. 8(a), then we affect the needed $Joint_5$ angle (Fig. 8(b)) and finally, we adapt $Joint_1$ and $Joint_3$ to the new circle using the same circles intersections equations in **Step-2** as illustrated in Fig. 8(c).

3.4.3. *Adding end-effector inertia (Whip Effect)*

The idea behind this effect is to add an intelligent control on the previous wrist movement ($Joint_5$), between a mechanical mode and an anthropomorphic mode. In the mechanical mode (left column in Fig. 9), the end-effector is the driving force of the movement. This seems normal as the sole objective of the robot arm movement is to make sure that the tool (the end-effector) achieves the target. At the same time, in the mechanical mode, the IK system tries to make the minimum possible movement

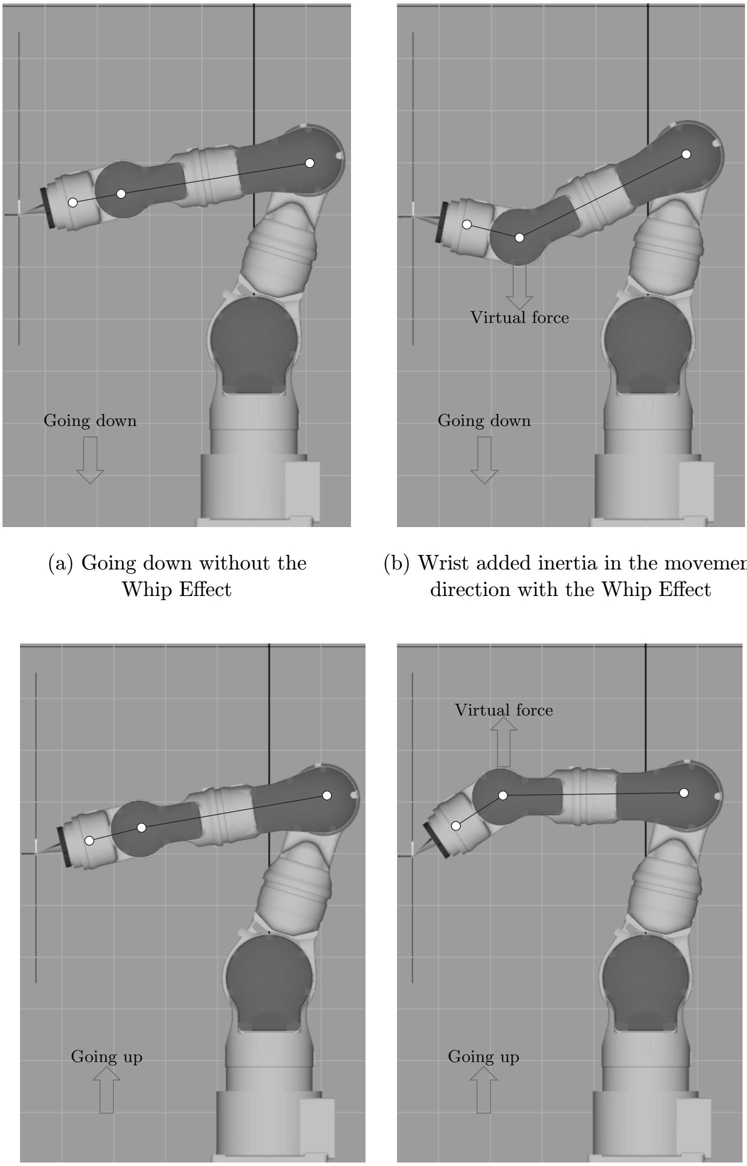

(a) Going down without the Whip Effect

(b) Wrist added inertia in the movement direction with the Whip Effect

(c) End-effector-based movement without Whip Effect during the rise

(d) Wrist added inertia in the movement direction

Fig. 9. Illustration of different configurations depending on if the effect is enabled or not.

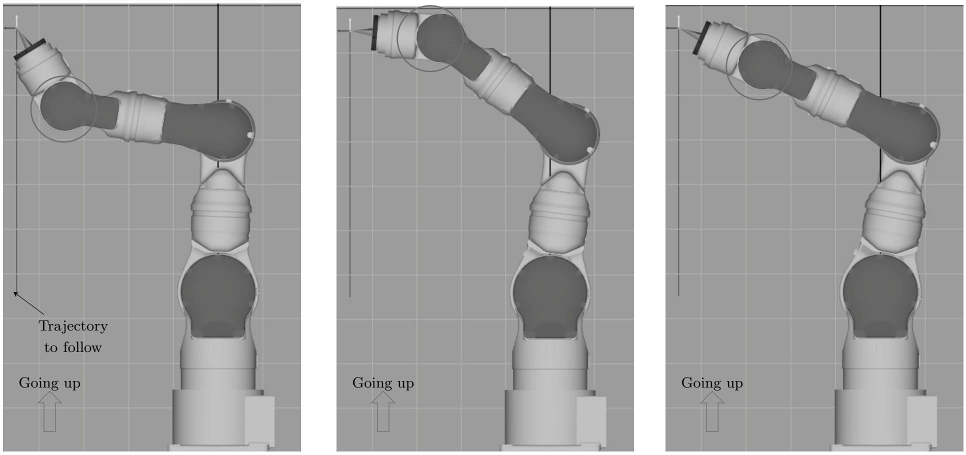

(a) End-effector-based movement without Whip Effect

(b) Wrist-based movement with whip effect

(c) Wrist-based movement in rest state (at the end of the movement)

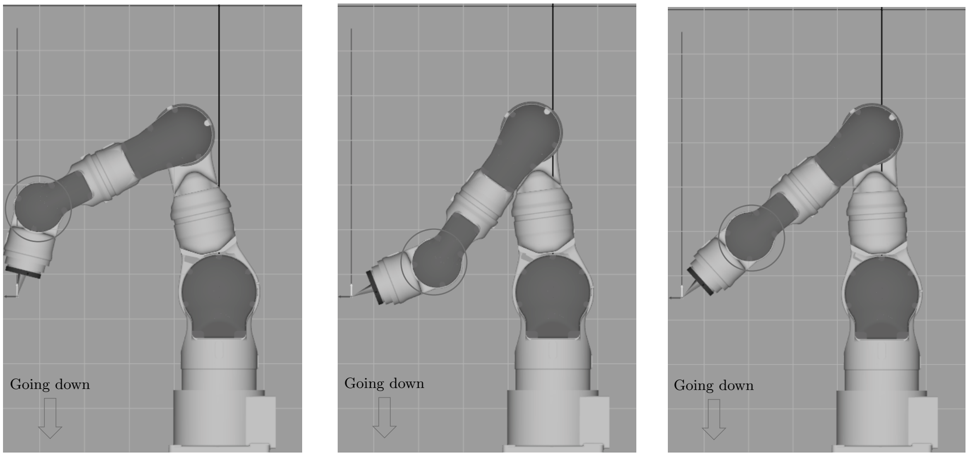

(d) End-effector-based movement without Whip Effect

(e) Wrist-based movement with whip Effect

(f) Wrist-based movement in rest state (at the end of the movement)

Fig. 10. Wrist spring damper reaches a rest state when the movement stops.

(moving the joints as minimum as possible) in order to simulate a robot that is looking for energy efficiency. In this mode, the robot tries to only move its wrist Joint_5 to achieve the target and the IK system adapts to this new wrist position. Only when the relative angle Joint_5 reaches a certain limit the rest of the joints start being more active and follows the end-effector.

In the anthropomorphic mode, we add an end-effector inertia (Whip Effect): We apply a virtual force on the wrist in the direction of the end-effector movement.

While we ensure that the end-effector reaches the target, we add an inertia component to the wrist making it the driving component of the movement. This effect can be observed when watching the wrist-brush movement of a painter or the movement of the wrist-equivalent joint in animals when running. We call it the **Whip Effect** because it resembles the wrist/whip movement when someone slings a whip: The tip of the whip is always in delay behind the rest of the whip until it reaches the target. And as we are going to see in this study, this movement is quite important when humans perceive the robot movement.

To add this effect, we calculate an angle θ_{w^1} based on the arm movement direction and we use a spring damper (the same type as before) to smooth this angle, given us a θ_{w^2} that we apply on Joint_5 (see Fig. 9 right column).

When the robot arm stops moving, the spring damper converges to its rest state giving us the positions in Figs. 10(c) and 10(f).

Both robotic and anthropomorphic wrist effects work in 3D by using 2 spring dampers: One on the pitch component of the movement affecting Joint_5 directly and a second one on the roll component of the movement affecting Joint_4 directly (see Fig. 11).

3.4.4. *Robots generalization*

Finally, we generalize this IK system on the other robots as follows:

(1) The 6-DOF robot can be seen as the same as the 7-DOF without Joint_2 of the 7-DOF robot.
(2) The 15-DOF robot is two 7-DOF arms with a common base Joint_0 that always tries to face the middle point of both arms target. We apply the **Base Inertia** on this joint.

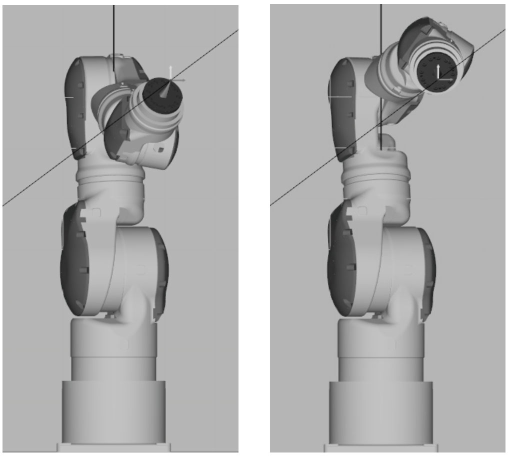

(a) Without Whip Effect (b) With Whip Effect

Fig. 11. Added effects on the Wrist in 3D.

4. User Study

4.1. *Aim of the study*

The aim of the study was to observe and compare different robot movements, to determine which criteria were perceived as human-like and to determine their correlation with other notions such as safety. In this context, a use case was chosen in which an industrial robot arm had to work on a car door according to different movement conditions. A within-subject study was performed with a diverse population: The users had to observe each movement condition and to give their feelings by answering a questionnaire.

4.2. *Use case*

The industrial use case we studied was a car door assembly. One important operation in this use case is the setting of a sealing sheet. This operation currently requires the operator to put a sealing sheet on the door, to ensure it is well positioned and to definitely stick it to the door by rolling a caster on the edges.

In our situation, an industrial robot arm (7-DOF Motoman SIA10 robot) was imagined to apply the caster on the edges of the sheet. The robot's end-effector travelled along its trajectory (the edges of the sheet) at about 0.4 m/s (see Fig. 12). The robot also had to stop at two specific points of the trajectory, since interesting behaviors (like inertia) may appear when the movement is stopped. The robot was performing its task in an infinite loop, to give time to the users to observe it.

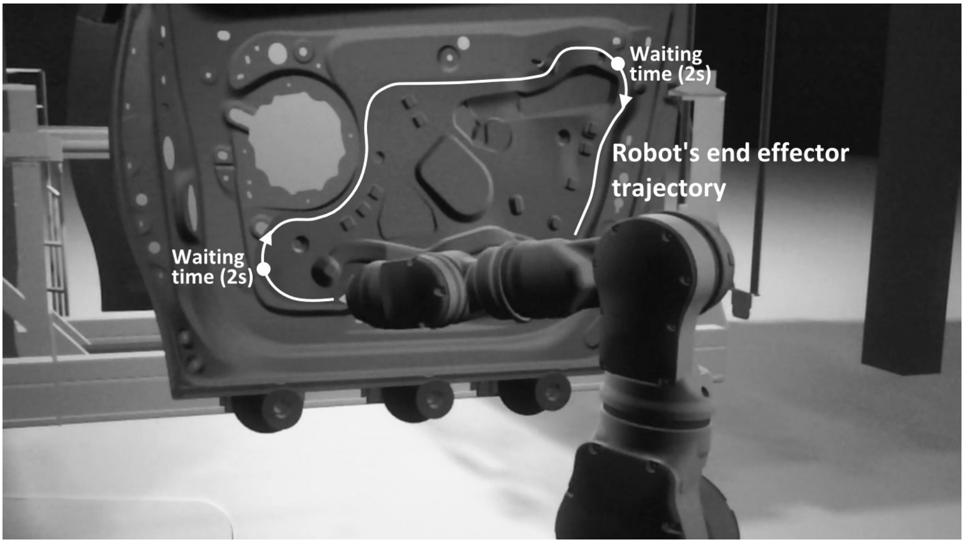

Fig. 12. The industrial use case: The setting of the sealing sheet.

4.3. *Robot movements*

The movements of the robot could vary depending on three main parameters, controlled by the tool described in Sec. 3. Table 1 shows details concerning these parameters. Parameter P_1 controlled the inertia on the robot's base, resulting in a delay between the base and the first segment of the robot. Parameter P_2 controlled the inertia on the end-effector. Parameter P_3 was used to modify the velocity profile (linear or two-thirds power law). Those parameters were inspired by biomechanics and chosen based on Spir.Ops experience in IK Systems. They were used to generate movements that were natural and plausible on robot arms, and were sufficient for our study. They were simple to use and allowed us to generate a large panel of movements that were quite different.

Given these three parameters, eight different types of robot movements were generated depending on the activation of each parameter. A reference movement (the other movements had to be compared to this one) was also designated, with all parameters deactivated. Table 2 shows the name of each robot condition and their corresponding parameter activation.

4.4. *Experimental setup*

The use case was implemented in a virtual environment using virtual reality. 3D models of the industrial environment were used: A car door, an assembly line and a robot. The virtual environment was rendered on a back-projected wall

Table 1. Parameters controlling the robot's movements.

Parameters	On	Off
P_1 Inertia on the base	1.5 s	0.05 s
P_2 Inertia on the end-effector	roll = 15	roll = 0
	pitch = 30	pitch = 0
P_2 Velocity profile	Two-thirds power law	Linear

Table 2. Robot movement conditions and their parameter activation.

Robots	P_1	P_2	P_3
R_{ref}	Off	Off	Off
R_0	Off	Off	Off
R_1	On	Off	Off
R_2	Off	On	Off
R_3	Off	Off	On
R_4	On	On	Off
R_5	Off	On	On
R_6	On	Off	On
R_7	On	On	On

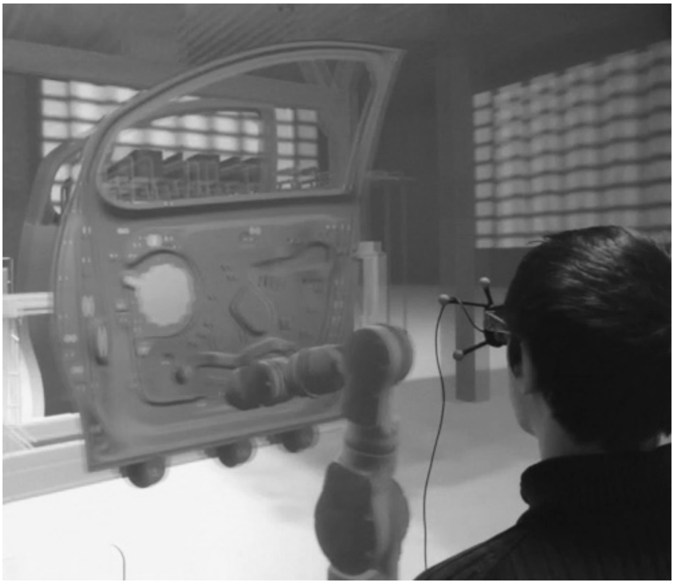

Fig. 13. A user in the virtual environment.

($3.1\,\mathrm{m} \times 1.7\,\mathrm{m}$) with active stereoscopy. ART cameras were used to track the head of the users (see Fig. 13).

4.5. *User study protocol*

The user test was conducted as follows. Each robot had to be compared with the reference one. Before each condition, R_{ref} was first shown to the users. When the participants had sufficiently observed the reference robot, the test robot was presented to them and R_{ref} disappeared. The participants took their time to perceive differences with the reference then said to the coordinator when they were ready to answer the questionnaire. After answering the questions, the reference robot was shown again and the test went on with the next robot movement.

The questionnaire is shown in Table 3. For each question, a 7-point Likert scale was used: The participants had to give a grade relative to the reference robot, between -3 and $+3$. If a difference was perceived in a negative manner, a negative grade could be given (-3, -2, -1); if a difference was perceived in a positive manner, a positive grade could be given (1, 2, 3); if no difference was perceived, a neutral grade could be given (0). The questionnaire was written with the help of a person from ergonomics. The construct validity of the questionnaire was, however, not checked.

The order of robot movements was randomized for each participant. Moreover, three occurences of robot R_0 (identical to R_{ref}) were presented (R_{01} being the first apparition, R_{02} the second one and R_{03} the last one), so that there were actually

Table 3. The questionnaire for each robot movement.

	Questions	Notions	Symbols
1	Does this robot seem controlled by a human or by a machine?	Humanlikeness	C_{h}
2	Does this robot seem more natural than the reference?	Naturalness	C_{n}
3	Does this robot seem more competent than the reference?	Competence	C_{c}
4	Does this robot seem more aggressive than the reference?	Aggressiveness	C_{a}
5	Does this robot seem more relaxing than the reference?	Relaxation	C_{r}
6	Does this robot seem more flexible than the reference?	Flexibility	C_{f}
7	Does this robot seem faster than the reference?	Speed	C_{s}
8	Does this robot seem more mechanical than the reference?	Mechanical	C_{m}
9	Does this robot seem more predictable than the reference?	Predictability	C_{p}
10	Do you feel safer next to this robot?	Safety	C_{sa}
11	Do you prefer this robot than the reference?	Preference	C_{pr}
12	Do you feel more stressed next to this robot?	Stress	C_{st}
13	Would you prefer to work next to this robot?	Work situation	C_{w}

10 robot conditions (R_{01}, R_{02}, R_{03}, R_1, R_2, R_3, R_4, R_5, R_6, R_7). The three robots R_0 were strictly identical to the reference R_{ref}. Each participant was aware of the fact that a robot could be identical to the reference but they did not know when such a robot appeared. The test stopped when all the robot conditions had been seen by the participant. The duration of the experiment for each subject was about 30 min.

4.6. *Population*

A total of 39 subjects participated in this study. The average age was 35.2 with a median of 31. There were 17 men and 22 women with a wide variety of working fields and study level (from no degree to Ph.D.). None of them were familiar with robots.

5. Results

In this section, we show and analyze the results of the questionnaire. First, we present an overview of the results by performing a comparison between movement parameters. Then, we propose an interpretation of the results of this comparison. Finally, we present the overall detailed results of the questionnaire, by notions and over all the robots.

5.1. *Parameter comparison*

In order to determine which parameters were responsible for the robot's human-likeness and other notions of the questionnaire, robots were grouped depending on their parameters. For each parameter (P_1, P_2, P_3), two groups were made: The robot conditions activating the corresponding parameter and the ones not activating it. Figures 14(a), 14(b) and 15 shows the average answers to the questionnaire for each subgroup of each parameter. Wilcoxon tests were performed to determine significant differences between subgroups. For robot R_0, only the last occurence R_{03} was taken into account.

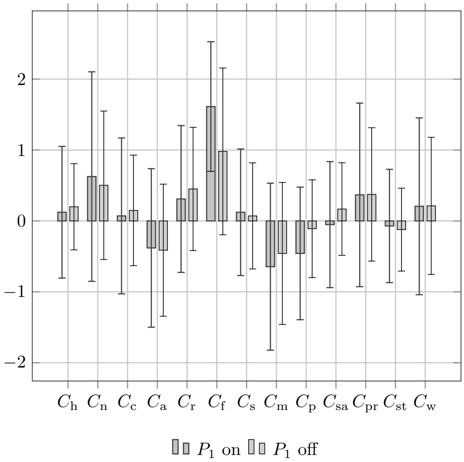

(a) Results depending on P_1

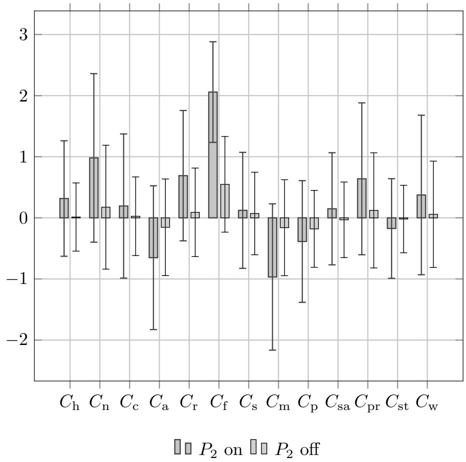

(b) Results depending on P_2

Fig. 14. Results depending on P_1 and P_2 activated or not.

As can be seen in Fig. 14(b), parameter P_2 seems to have the most influence in the perception of robot movements. Indeed, no significant difference was found between subgroups for parameter P_3 (Fig. 15), meaning that velocity profile was of little impact. Significant differences were found for P_1 only for flexibility, mechanicality and predictability (Fig. 14(a)), while for P_2 significant differences were found for every notion of the questionnaire, except competence, speed, and stress. This shows that the important parameters in the perception of robot movements are, in decreasing importance order, P_2, P_1 and then P_3.

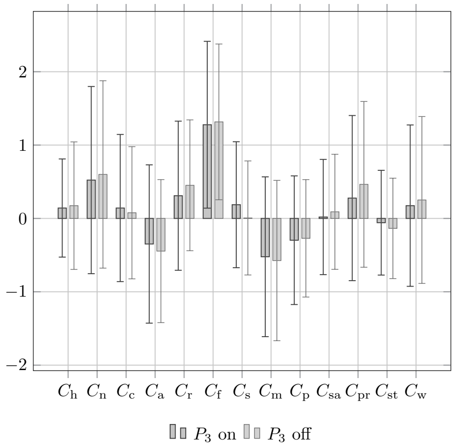

Fig. 15. Results depending on P_3 activated or not.

Table 4. Calculations of ΔP_1 and the corresponding states of the other parameters. Similar calculations were performed for ΔP_2 and ΔP_3.

ΔP_1	P_2 state	P_3 state
R_1-R_0	Off	Off
R_4-R_2	On	Off
R_6-R_3	Off	On
R_7-R_5	On	On

In order to study the interaction effects between parameters, we conducted an additional analysis. The aim of this analysis was to evaluate whether the influence of a specific parameter (P_1, P_2, or P_3) depended on the states of the other parameters (activated or not). In the following, we define the influence of a specific parameter P_i as the difference ΔP_i in grades between a robot having P_i activated and the same robot having P_i deactivated (see Table 4 for the calculations with parameter P_1). Having significant different values of ΔP_i when another parameter P_j is activated and when P_j is deactivated shows that there is a significant interaction effect between P_i and P_j. Wilcoxon pairwise tests were performed to compare each category and assess significant differences.

The results showed no significant interaction effect between parameters P_1 and P_3 and between parameters P_2 and P_3. This is mainly due to the already nonexistent influence of parameter P_3 on the results. However, a significant interaction effect was shown between P_1 and P_2, for all notions except competence, speed, predictability and work situation. Figure 16(a) shows the comparison of results for ΔP_1 when P_2 is

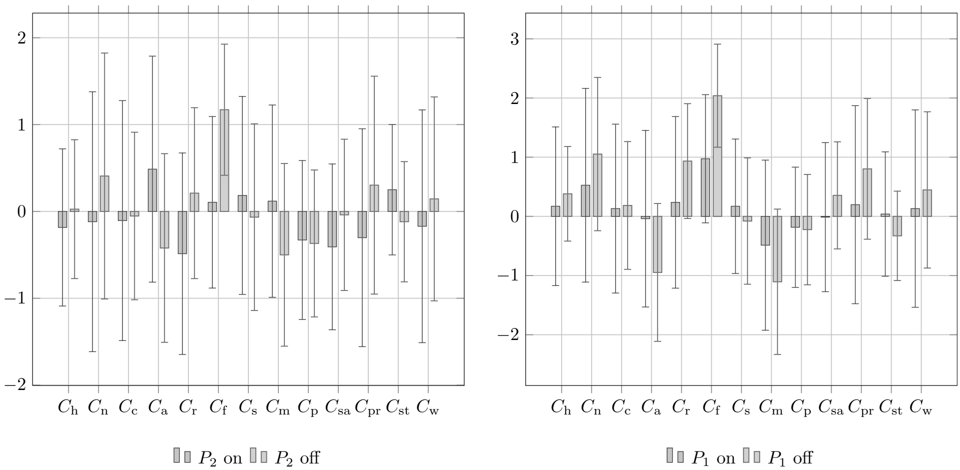

(a) Values of ΔP_1 depending on P_2

(b) Values of ΔP_2 depending on P_1

Fig. 16. Influences of parameters P_1 and P_2 (ΔP_1 and ΔP_2) depending on the other parameter's state.

activated and deactivated, while Fig. 16(b) shows the comparison of results for ΔP_2 when P_1 is activated and deactivated.

In Fig. 16(a), we can clearly see that the influence of parameter P_1 (ΔP_1) was different depending on if P_2 was activated or not. The difference is mostly qualitative: While a certain trend for ΔP_1 was shown when P_2 was deactivated, the opposite trend was shown when P_2 was activated. On the whole, the influence of P_1 was more positive when P_2 was deactivated, and the influence of P_1 became negative when P_2 was activated. For example, for aggressiveness, a positive influence of P_1 was shown when P_2 was deactivated ($\Delta P_1 < 0$, less aggressiveness was found), while the opposite trend appeared when P_2 was activated ($\Delta P_1 > 0$, more aggressiveness was found). Similar trends may be observed with the other notions of the questionnaire.

Significant differences were also found for ΔP_2 depending on the activation of P_1, but these differences were mostly quantitative (and not qualitative, see Fig. 16(b)). Indeed, the same trends were always observed for the influence of P_2 (positive influence), but with different amplitudes depending on the activation of P_1. The positive influence of P_2 was always more important when P_1 was deactivated than when P_1 was activated. This effect seems understandable: The influence of P_2 could be more clearly observed when there were no other parameters activated. When P_1 was activated, the movements were already perceived as more natural, thus decreasing the influence of P_2.

The analysis of the interaction effects shows that the results are always better when P_2 is activated. However, an interaction effect exists between P_1 and P_2 and shows that it may not be a good solution to have both P_1 and P_2 activated at the same time: The influence of P_1 would then be perceived in a negative way. Figure 17

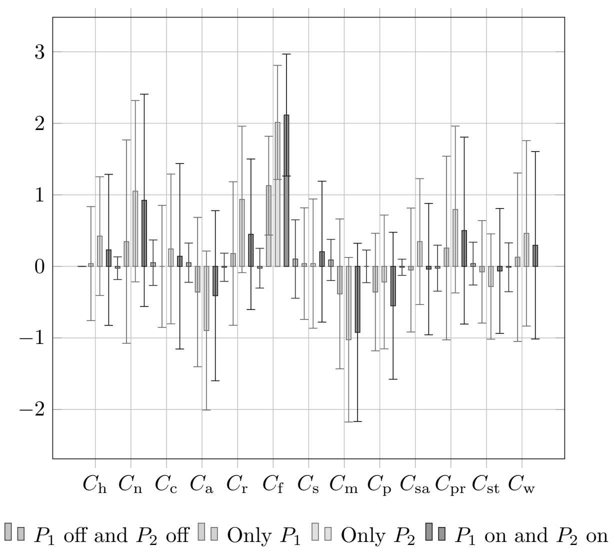

Fig. 17. Results depending on P_1, P_2 and their interaction.

shows the absolute results for four subgroups of robots: The ones having neither P_1 nor P_2 activated, the ones having only P_1 activated, the ones having only P_2 activated and the ones having both P_1 and P_2 activated. In this figure, we can clearly see that P_2 was responsible for the main differences in the perception of robot movements: Having P_2 alone activated was often an asset for a movement to be perceived as human-like and safe, while P_1 was of much more negligible or negative impact.

5.2. *Overall interpretation*

5.2.1. *Robot characteristics*

Three characteristics seemed to be common to the robots with P_2 activated (with P_1 or not): Flexibility, naturality and mechanicality. Indeed, for all three notions, those robots got the best grades. This shows that inertia on the end-effector of the robot was perceived as a mark of flexibility, and that a flexible robot was seen as more natural and less mechanical.

Moreover, three other characteristics were common only to the robots with P_2 alone activated: Human-likeness, aggressiveness and relaxation. For those notions, robots with only P_2 activated got better results than the robots with both P_1 and P_2 activated. The inertia of the end-effector was perceived as less aggressive (thus more relaxing) and more human-like, but it was the case only if P_1 was deactivated: Having both inertia on the base and on the end-effector was more negative than having inertia on the end-effector only.

Finally, robots with only P_2 activated were perceived as less predictable than the ones with P_1 activated. The inertia on the root implied more predictability: This can explain why it was perceived as less human-like and more aggressive.

5.2.2. *Users' feelings*

Regarding the last four notions on the users' feelings (safety, preference, stress, and work situation), robots with only P_2 activated always got the best results. The characteristics of flexibility and naturality could be used to explain this trend, but this would not explain the differences with the robots with both P_1 and P_2 activated. Therefore, it is the notions of human-likeness and aggressiveness that can explain this trend. Since the movements with P_2 alone activated were perceived as the least aggressive and the most relaxing, it is understandable that they induced less stress and more safety. Human-likeness also played a role in the users' feelings, especially to explain their preference and their will to work next to them.

5.3. *Results description with all the robots*

This section presents the results of the questionnaire, for each robot instead of each parameter. The aim is not to give a further analysis of the results: The main detailed analysis was given in Sec. 5.1, by comparing parameters. The aim is rather to give the detailed answers to the questionnaire and to illustrate the analysis from Sec. 5.1 by

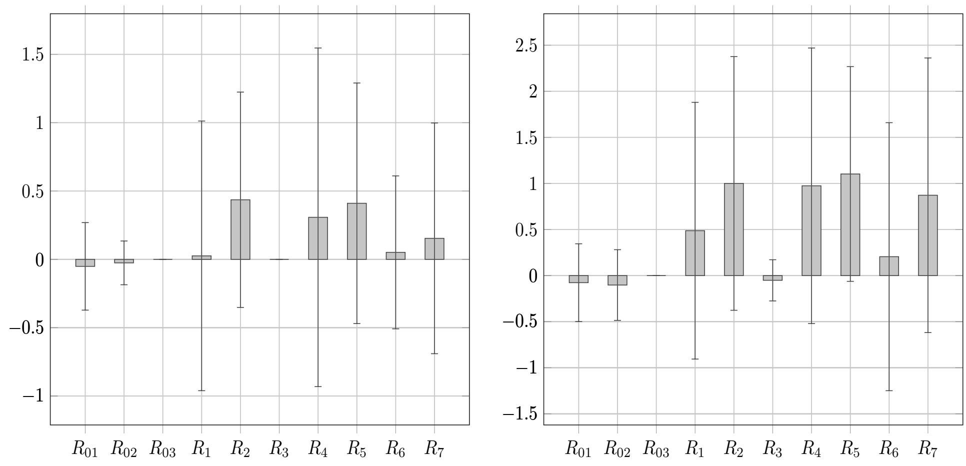

(a) Human–machine notion

(b) Natural–unnatural notion

Fig. 18. Results of the human-likeness and natural notions.

describing the results with an overview of all the robots. Figures 18–24 present the results of every notion of the questionnaire with each robot.

First, we can clearly observe that robots R_{01}, R_{02} and R_{03} were perceived close to the reference robot. This reflects that participants were clearly able to detect that a robot was similar to the reference, thus validating that they did not answer at random.

The relative importance of each parameter $(P_1,\ P_2,\ P_3)$ may be observed by simply comparing robots R_1, R_2, and R_3. R_3 was always rated close to the reference,

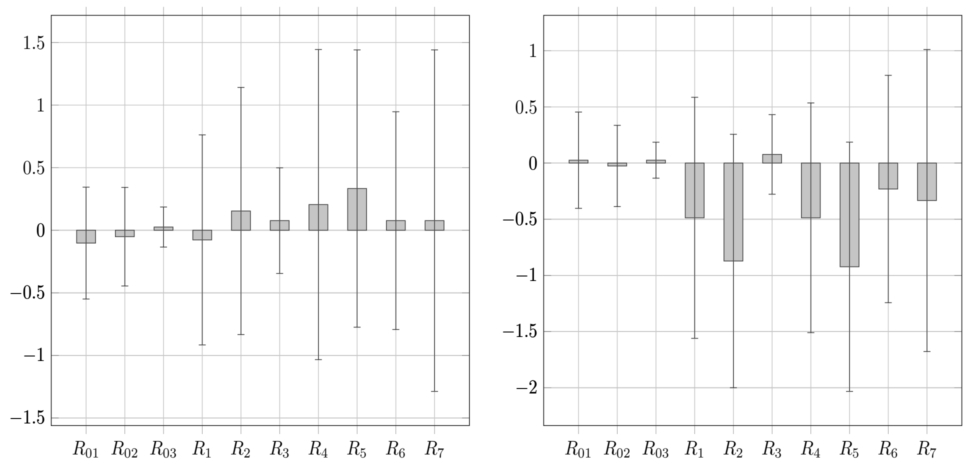

(a) Competent–incompetent notion

(b) Aggressive–harmless notion

Fig. 19. Results of the Competence and aggressiveness notions.

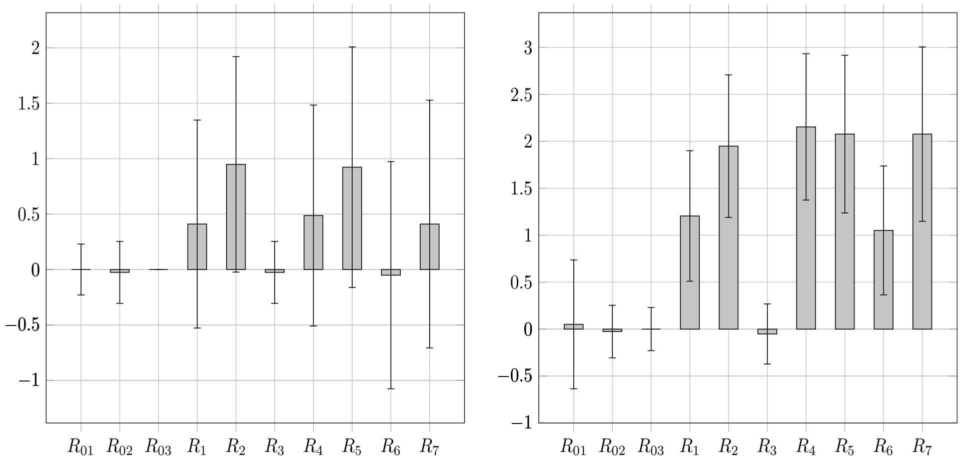

(a) Relaxing–soothing notion

(b) Flexible–tough notion

Fig. 20. Results of the relaxation and flexibility notions.

illustrating a low influence of parameter P_3, while R_2 always had the best results, illustrating a major influence of parameter P_2 compared to P_1.

It was shown in Sec. 5.1 that parameter P_3 had very little impact on the results of the questionnaire and on the other parameters. This can be observed in Figs. 18–24 by comparing robots and by forming pairs: R_0 and R_3, R_1 and R_6, R_2 and R_5, R_4 and R_7. Each of these pairs contain the same two robots, with or without P_3 activated. It is interesting to observe, for each notion of the questionnaire, that the two robots of

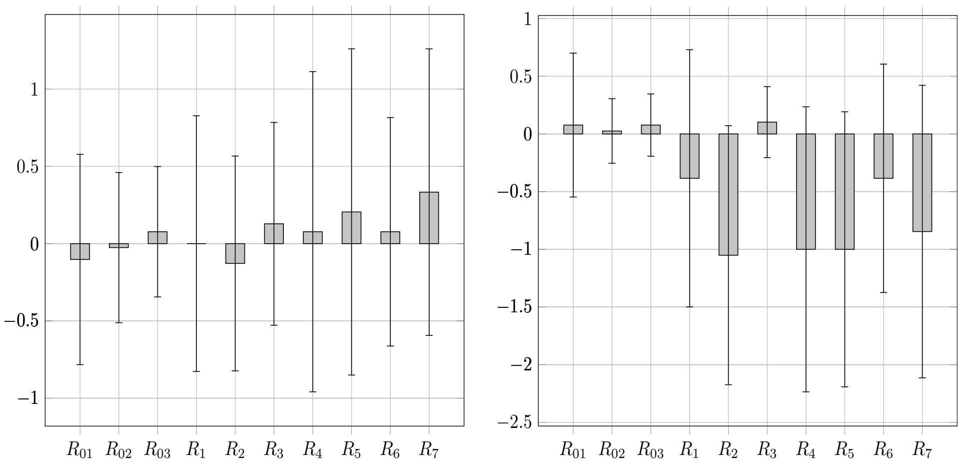

(a) Fast–slow notion

(b) Mechanical–nonmechanical notion

Fig. 21. Results of the speed and mechanical notions.

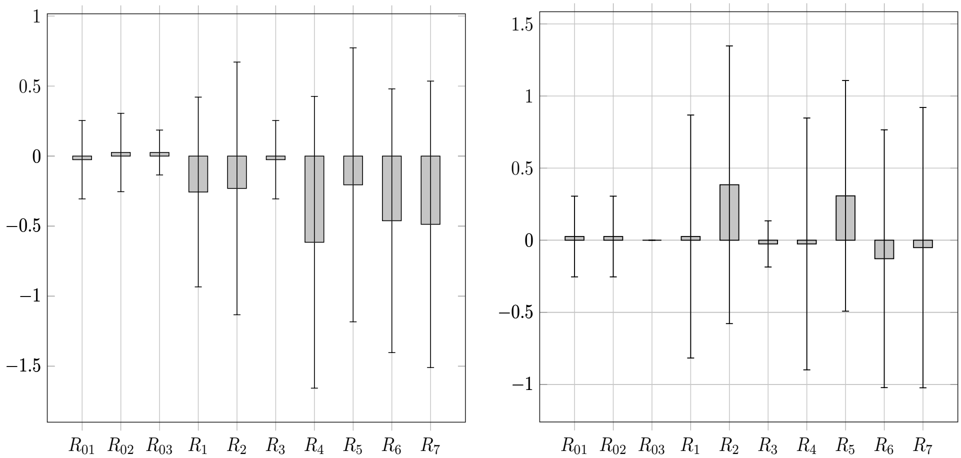

(a) Predictable–unpredictable notion

(b) Security–insecurity notion

Fig. 22. Results of the predictability and safety notions.

each pair were very often rated the same. This illustrates that parameter P_3 had little influence on the results.

Finally, it was also shown in Sec. 5.1 that parameter P_2 had the most influence on the results, but that it interacted with parameter P_1. The conclusion was that, to improve the user's feelings, it was better to activate P_2 alone rather than having both P_1 and P_2 activated. This conclusion may be observed in Figs. 18–24. Indeed, the pair of robots $R_2 - R_5$ had very often the best grades: This pair correspond to the robots having P_2 activated (but not P_1). The second pair of robots which had good

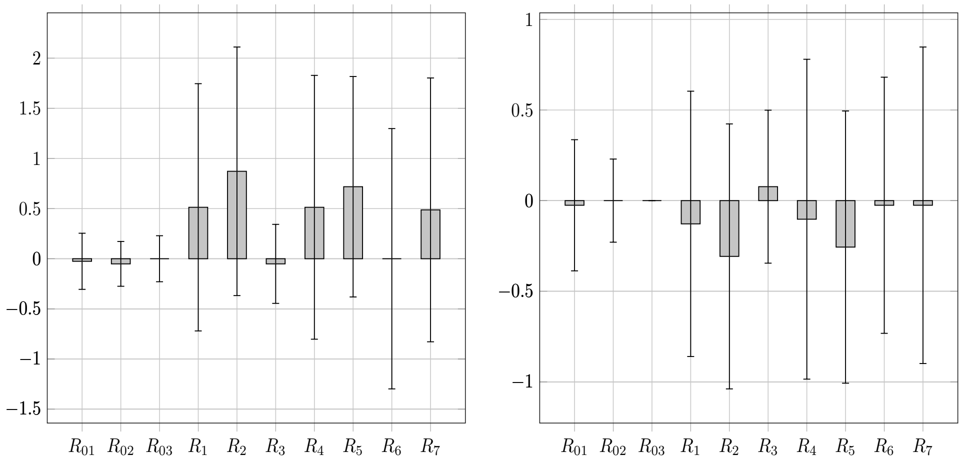

(a) Overall–preference notion

(b) Stress–nostress notion

Fig. 23. Results of the preference and stress notions.

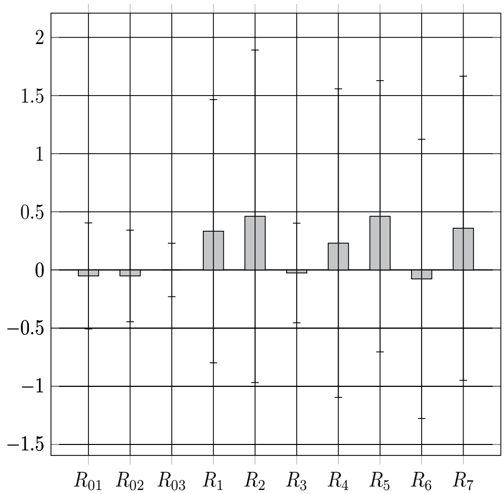

Fig. 24. Results of the work situation notion.

results (as good as or lower than the pair $R_2 - R_5$) in the questionnaire is the pair $R_4 - R_7$: This pair correspond to the robots having both P_1 and P_2 activated. Finally, the pair $R_1 - R_6$ correspond to the robots having P_1 activated (and not P_2) and always got lower results. This observation illustrates the conclusions given in Sec. 5.1. In the overall results shown in Figs. 18–24, we can observe that robot R_3 was approximately noted as the reference (notes are close to 0). This observation leads us to say that R_2 and P_3 had the greatest influence on this notion.

6. Conclusion

In this paper, the focus was to study the perception of robot movements. We were interested in evaluating what made robot movements human-like and in assessing people subjective opinions about it. In this context, different levels of anthropomorphic robot movements were generated thanks to an anthropomorphic IK system. A user study was conducted to compare several movements and gather subjective impressions about them. This user study relied on an industrial use case: An industrial robot arm had to perform a task on a car door in the context of an assembly line. This use case was implemented using virtual reality with a virtual robot. Questionnaires were given to the users to assess their impressions.

The results showed that the most important criterion of the robot movement was the inertia on the end-effector. Additionally to being perceived as more flexible and more natural, the inertia on the end-effector was also necessary for the movement to be perceived as more human-like and less aggressive. A further analysis showed that those two characteristics (human-likeness and aggressiveness) were essential in the users' feelings: A human-like and nonaggressive robot movement helped the users feel safer, less stressed and more willing to work with the robot.

These results may be used to design new robot movements that are better perceived by users in their environment. However, some care must be taken when analyzing our study. First, we did not check the construct validity of our questionnaire: This is a limitation of our study and we will focus on this issue for future studies. Secondly, our study was performed with a virtual robot: Results may change when dealing with a physical robot, especially concerning safety. Finally, the context of our study was a robot working on an industrial assembly line: Results should be extended to other situations (homecare robots for example) with caution. Imposing inertia on the robot end-effector may not always be possible, in cases where it has to keep a specific orientation. In spite of those remarks, we believe that our study improved the overall knowledge on the perception of robot movements.

Acknowledgments

We would like to thank all the subjects who gave their time to participate in the user study. This research benefited from the support of the Chair "PSA Peugeot Citroën — Robotics and Virtual Reality", led by MINES ParisTech and supported by S. A. Peugeot. The partners of the Chair cannot be held accountable for the content of this paper, which engages the authors' responsibility only.

References

1. T. W. Fong, I. Nourbakhsh and K. Dautenhahn, A survey of socially interactive robots, *Robot. Auton. Syst.* **1** (2003) 143–166.
2. A. Bauer, D. Wollherr and M. Buss, Human-robot collaboration: A survey, *Int. J. Hum. Robot.* **5**(1) (2008) 47–66.
3. D. Li, P. Rau and Y. Li, A cross-cultural study: Effect of robot appearance and task, *Int. J. Social Robot.* **2**(2) (2010) 175–186.
4. L. Saab, P. Souères, N. Mansard and J. Y. Fourquet, Generation of human-like motion on anthropomorphic systems using inverse dynamics, *Comput. Methods Biomech. Biomed. Eng.* **15**(1) (2012) 156–158.
5. W. Suleiman, E. Yoshida, F. Kanehiro, J.-P. Laumond and A. Monin, On human motion imitation by humanoid robot, *IEEE Int. Conf. Robotics and Automation, ICRA 2008,* May 2008, pp. 2697–2704.
6. G. Simmons and Y. Demiris, Biologically inspired optimal robot arm control with signal-dependent noise, *in Proc. 2004 IEEE/RSJ Int. Conf., Intelligent Robots and Systems, 2004. (IROS 2004)*, Vol. 1 (IEEE, 2004), pp. 491–496.
7. D. S. Syrdal, K. Dautenhahn, S. N. Woods, M. L. Walters, and K. L. Koay, Looking good? Appearance preferences and robot personality inferences at zero acquaintance, technical report in *Proc. AAAI Summer Symp. on Multidisciplinary Collaboration for Socially Assistive Robotics AAAI* (2007).
8. S. Shibata and H. Inooka, Psychological evaluations of robot motions, *Int. J. Ind. Ergon.* **21**(6) (1998) 483–494.
9. B. R. Duffy, Anthropomorphism and the social robot, *Robot. Auton. Syst.* **42**(3–4) (2003) 177–190.
10. K. Khalaf and H. Hemami, The past and present of human movement research: Towards the disign of human-like robots, *J. Mech. Med. and Biol.* **12**(02) (2012) 1240005.

11. M. Mori, The uncanny valley, *Energy* **7** (1970) 33–35.
12. A. Stenzel, E. Chinellato, M. A. T. Bou, Á. P. del Pobil, M. Lappe and R. Liepelt, When humanoid robots become human-like interaction partners: Corepresentation of robotic actions, *J. Exp. Psychol, Hum. Percept. Perform.* **38** (2012) 1073–1077.
13. P. Morasso, Spatial control of arm movements, *Exp. Brain Res.* **2** (1981) 223–227.
14. P. Viviani and C. Terzuolo, Trajectory determines movement dynamics, *Neurosci.* **7**(2) (1982) 431–437.
15. G. Johansson, Visual perception of biological motion and a model for its analysis, *Atten. Percept. Psychophysi.* **14** (1973) 201–211, doi: 10.3758/BF03212378.
16. T. Flash and N. Hogan, The coordination of arm movements: An experimentally confirmed mathematical model, *J. Neurosci.* **5** (1985) 1688–1703.
17. Y. Uno, M. Kawato and R. Suzuki, Formation and control of optimal trajectory in human multijoint arm movement, *Biol. Cybern.* **61** (1989) 89–101.
18. S. Gibet, J.-F. Kamp and F. Poirier, *Gesture Analysis: Invariant Laws in Movement* (Springer, Berlin, Heidelberg, 2004), pp. 1–9.
19. M. Taïx, M. T. Tran, P. Souères and E. Guigon, Generating human-like reaching movements with a humanoid robot: A computational approach, *J. Comput. Sci.* **4**(4) (2013) 269–284.
20. M. Huber, M. Rickert, A. Knoll, T. Brandt and S. Glasauer, Human–robot interaction in handing-over tasks, *17th IEEE Int. Symp. Robot and Human Interactive Communication, 2008, RO-MAN 2008.* August 2008, pp. 107–112.
21. D. Kulić and E. Croft, Affective state estimation for human-robot interaction, *IEEE Trans. Robotics* **23** (2007) 991–1000.
22. A. M. Zanchettin, L. Bascetta and P. Rocco, Acceptability of robotic manipulators in shared working environments through human-like redundancy resolution, *Appl. Ergon.* **44**(6) (2013) 982–989.
23. V. Weistroffer, A. Paljic, L. Callebert and P. Fuchs, A methodology to assess the acceptability of human-robot collaboration using virtual reality, in *VRST'13: Proc. 19th ACM Symp. Virtual Reality Software and Technology* (ACM, New York, NY, USA, 2013) pp. 39–48.
24. F. E. Pollick, J. G. Hale and M. Tzoneva-Hadjigeorgieva, Perception of humanoid movement, *Int. J. Hum. Robot.* **2**(3) (2005) 277–300.
25. M. Salem, F. Eyssel, K. Rohlfing, S. Kopp and F. Joublin, To err is human(-like): Effects of robot gesture on perceived anthropomorphism and likability, *Int. J. Social Robot.* **5**(3) (2013) 313–323.
26. H. van Welbergen, B. J. H. van Basten, A. Egges, Z. Ruttkay and M. H. Overmars, Real time animation of virtual humans: A trade-off between naturalness and control, *Comput. Graph. Forum* **29**(8) (2010) 2530–2554.
27. M. Girard and A. A. Maciejewski, Computational modeling for the computer animation of legged figures, in *Proc. 12th Annual Conf. Computer Graphics and Interactive Techniques, SIGGRAPH '85* (New York, NY, USA) (ACM 1985), pp. 263–270.
28. M. Girard, Interactive design of 3D computer-animated legged animal motion, in *Proc. 1986 Workshop on Interactive 3D Graphics, I3D'86* (New York, NY, USA) (ACM, 1987), pp. 131–150.
29. D. G. Luenberger, *Linear and Nonlinear Programming.* (Addison-Wesley, 1984).
30. L. C. T. Wang and C. C. Chen, A combined optimization method for solving the inverse kinematics problems of mechanical manipulators, *IEEE Trans. Robot. Autom.* **7**(4) (1991) 489–499.
31. K. Grochow, S. L. Martin, A. Hertzmann and Z. Popović, Style-based inverse kinematics, *ACM Trans. Graph.* **23** (2004) 522–531.

32. M. Kallmann, Analytical inverse kinematics with body posture control, *Comput. Animat. & Virtual Worlds* **19** (2008) 79–91.
33. X. Wu, M. Tournier and L. Reveret, Natural character posing from a large motion database, *IEEE Comput. Graph. Appl.* **31** (2011) 69–77.
34. L. Kovar and M. Gleicher, Automated extraction and parameterization of motions in large data sets, in *ACM SIGGRAPH 2004 Papers, SIGGRAPH'04* (New York, NY, USA) (ACM, 2004), pp. 559–568.
35. R. W. Sumner, M. Zwicker, C. Gotsman and J. Popović, Mesh-based inverse kinematics, *ACM Trans. Graph.* **24** (2005) 488–495.
36. K. G. Der, R. W. Sumner and J. Popović, Inverse kinematics for reduced deformable models, in *ACM SIGGRAPH 2006 Papers, SIGGRAPH'06* (New York, NY, USA) (ACM, 2006), pp. 1174–1179.
37. A. A. Karim, T. Gaudin, A. Meyer, A. Buendia and S. Bouakaz, Adding physical like reaction effects to skeleton-based animations using controllable pendulums in *Transactions on Edutainment VI*, Vol. 6758 (Springer-Verlag, 2011), pp. 111–121.

Olivier Hugues received his Ph.D. from the University of Bordeaux I (Aquitaine, France) in the field of information technology. He then worked at the Université du Québec en Abitibi-Témiscamingue (QC, Canada) in the mining sector and, subsequently, served as Assistant Professor in MINES ParisTech's Robotics Lab in the "Virtual Reality & Augmented Reality" team. One of his main interests is the understanding of augmented reality from the user point of view. He is also involved in the field of human-robot collaboration.

Vincent Weistroffer was a Ph.D. student at the Centre for Robotics, Mines ParisTech, within the chair "PSA Peugeot Citroën — Robotics and Virtual Reality" and received his Ph.D. degree in 2014. His topics of interest include the acceptability of human-robot collaboration, from the point of view of operators, and the use of virtual reality to simulate such work situations. Vincent Weistroffer now works in the Interactive Simulation Lab (LSI) at CEA-LIST where he studies the same topics for industrial applications.

Alexis Paljic is an assistant professor in MINES ParisTech's Robotics lab, he conducts research on Immersion and Interaction within Virtual Environments in the context of industrial uses of VR. One of his main interests is the question of the representativity of human activities within Virtual Environments compared to their Real Counterparts.

Philippe Fuchs, Ph.D., Professor in Mines ParisTech engineering school (Paris) is the leader of "Virtual Reality & Augmented Reality" team. The field of his research is the theoretical approach of VR and industrial applications. He is author and coordinator of 6 books, 13 chapters of other books, 26 articles of international journals, 54 articles in international congress with selection committee review and 28 other articles.

Ahmad Abdul Karim has a Ph.D. in procedural animation of characters/creatures from Lyon 1 University, LIRIS laboratory. His Ph.D. was a collaboration between SAARA Group: Simulation, Analysis and Animation for Augmented Reality and Spir.Ops: a Private Scientific Research Lab focused on Artificial Intelligence issues. He has completed his masters in Artificial Intelligence from Toulouse 3 University. Currently he is an R&D Engineer in the Animation Team at Spir.Ops. His current research interests include AI-Driven character animations, real-time systems and most importantly procedural animation.

Thibaut Gaudin Received his Master Degree of Engineering from the French Graduate Engineering School ESIEA in 2000. Has a French Master degree in Simulation and Virtual Reality from the French Engineer School Arts et Métiers ParisTech in 2001. Specialized in procedural character animation, he worked as an R&D Engineer and as a freelance for different research lab and companies (LAAS-CNRS, DURAN R&D, Nicephore City, Xtranormal). Since 2009, he is an R&D Engineer for the French company Spir.Ops: a Private Scientific Research Lab. Procedural character animation is still his main interest.

Axel Buendia is one of the founders of Spir.Ops, a company which provides advanced AI services and tools. A Ph.D. and several years working for different video game studios, such as Cryo, Polygon Studios, gave him the experience to create advanced tools to design next gen behaviors. Since the creation of Spir.Ops, he has worked with well known companies such as Ubisoft, and on different styles of games, from sport to FPS and adventure. As a middleware provider, Spir.Ops is aware of the latest needs of most video game projects, and try to anticipate their wish. Having projects on DS, PC, PS3, XBox360, we have a great experience of AI platform dependencies.